

Gas Sorption and the Consequent Volumetric and Permeability Change of Coal I: Experimental

Wenjuan Lin · Anthony R. Kovscek

Received: 20 December 2013 / Accepted: 4 August 2014 / Published online: 20 August 2014
© Springer Science+Business Media Dordrecht 2014

Abstract Experimental and numerical investigations were conducted to study adsorption and desorption of pure and multicomponent gas on coal, and the sorption-induced volumetric strain and permeability change of the coal. This paper presents the experimental work. Using CO₂, N₂, and CO₂ and N₂ binary mixtures of different composition as injection gases, the measurements were conducted on a cylindrical composite coal core at varying pore pressures and constant effective confining pressure. Sorption was measured using a volumetric method. The initial and equilibrium system pressure and gas phase composition were measured. The total amount of adsorption and the composition of the adsorbed phase (for adsorption of binary gas mixtures) were calculated based on material balance. During the process of sorption, the volume of the core was monitored by recording the volume of the water in the confining pressure vessel. Sorption-induced strain was calculated as the ratio of the sorption-induced volumetric change to the initial volume of the core. After adsorption equilibrium was reached, the permeability of the core was measured based on the Darcy equation for gas flow. Sorption and permeability measurements were conducted for each test gas at first increasing and then decreasing pressures. Volumetric strain was only measured while pore pressure increased. To our knowledge, this is the first study measuring adsorption, volumetric strain, and permeability on the same piece of core with the same apparatus.

Keywords Coalbed methane · Permeability evolution · Gas adsorption · Sorption-induced volumetric strain

W. Lin
Chevron Energy Technology Company, Houston, TX, USA
e-mail: wenjuanlin5@gmail.com

A. R. Kovscek (✉)
Energy Resources Engineering Department, Stanford University, Stanford, CA, USA
e-mail: kovscek@stanford.edu

1 Background

Coalbed methane is the name for natural gas in underground coal seams. Almost all coal seams contain some gas that was generated during the coalification process, either from a biological process as a result of microbial action or from a thermal process as a result of increasing temperature with the burial of the coal (Thomas 2002). The gas is mainly methane with various amounts of other components including ethane, propane, carbon dioxide, nitrogen, helium, and hydrogen (British Geological Survey 2006). Gas in coal was historically considered a hazard due to the risks of explosions and outbursts associated with coal mining. From the 1980s, however, coalbed methane began to be recognized as a fuel that produces comparatively less CO₂ than other fossil fuels. According to the U.S. Energy Information Administration, coalbed methane accounted for about 8.5 % of the United States dry natural gas production in 2010.

Different from conventional natural gas in sandstone reservoirs that exists mainly as free gas in the pore spaces, gas in coal mainly exists as an adsorbed phase on the internal surface area of the coal (Gray 1987). The amount of gas retained by coal is a function of the reservoir pressure and temperature, and the mineral content and structure of the coal (Thomas 2002). Coal seams are often saturated with formation water. Methane is held in place by the water pressure, until certain conditions are satisfied, for instance, a decrease in the reservoir pressure or the presence of a more adsorbing gas. Currently, coalbed methane is produced mainly through primary recovery by reservoir depressurization. Large volumes of formation water are pumped out from the reservoir, reservoir pressure decreases, methane desorbs from the internal coal surfaces, concentrates in the coal seams, migrates toward the wellbore, and then flows up to the ground surface through the wellbore annulus. Primary recovery is straightforward to implement, however, it leaves more than half of the resource behind. The large amount of produced water also poses many environmental concerns. Injection of nitrogen, carbon dioxide, or mixtures of the two was shown to be an effective technique to improve the ultimate recovery of coalbed methane in laboratories (Jessen et al. 2008). With the injection of nitrogen, the partial pressure of methane in the coal seams decreases, causing methane to desorb from the coal surfaces. In the case of carbon dioxide injection, carbon dioxide replaces methane on the coal surfaces because coal has stronger affinity for carbon dioxide than methane. Methane is produced and carbon dioxide remains in the coal seams that serves as a means of greenhouse gas sequestration.

Coalbed methane reservoirs are characterized as naturally fractured, dual porosity, and low permeability (Jahediesfanjani and Civan 2005). Figure 1 is a picture of one piece of the coal used in our study. Coal has a matrix-fracture structure. Micro pores in the matrices account for the majority of the porosity and are the major residences of the gas in coal. The natural fracture/cleat network accounts for most of the permeability for fluid flow in the reservoirs. It is observed that the permeability of coal changes with gas production/injection. Two mechanisms are believed to cause the permeability change (Harpalani and Zhao 1989): (1) change of effective stress and (2) volumetric strain caused by gas desorption/adsorption. For instance, during the primary recovery process, as gas is produced, the reservoir pressure decreases; effective stress on the reservoir formation increases assuming the overburden pressure does not change. Consequently, reservoir permeability decreases due to compression and closure of fractures and cleats, Fig. 2a. Meanwhile, as the reservoir pressure decreases, gas releases from the matrices of the coal causing shrinkage, thus the opening of cleats and an increase in permeability, Fig. 2b. According to the theory of physical adsorption, the process of adsorption causes a reduction in the free surface energy of the adsorbent that caused a proportional expansion of the adsorbent (Ares and Barron 1998). Desorption, on the other

Fig. 1 A coal sample from Wyodak-Anderson coal zone, Powder River Basin, Montana



hand, could cause an opposite effect, i.e., shrinkage of adsorbent. The adsorbent in this case is the coal. The actual permeability change in the field is a result of the two competing effects. Both permeability increase and reduction were observed (Gray 1998).

2 Laboratory Techniques for Permeability, Adsorption, and Strain Measurements on Coal

In the past four decades, many researchers measured coal permeability, gas adsorption on coal, and strain of coal in laboratories (Pan and Connell 2012; Talu 1998). Besides the general considerations in conducting these measurements, experiments with coal pose more challenges due to the following reasons: (i) coal is easy to break and specimens are hard to prepare, (ii) coal has very low permeability, and (iii) the amount of adsorption is not only a function of the pressure and temperature, but also depends on the mineral content and structure of the coal.

Relevant to gas production and injection in coalbed methane reservoirs and CO₂ sequestration in coal, the gas permeability of coal usually needs to be determined. In the laboratory, permeability is measured using either the Darcy equation for gas flow at steady state or the transient pressure transfer equation. When the Darcy equation is used, the permeability is measured by flowing gas through the core under a pressure gradient (Lin et al. 2008). The upstream and downstream pressures and the gas flow rate are measured. The permeability is calculated based on Darcy's law applied to a compressible system of finite length (Katz and Lee 1990).

$$k = \frac{2\mu_g q_a p_a L}{A (p_1^2 - p_2^2)}, \quad (1)$$

where k is the permeability of the specimen, μ_g is the viscosity of the flowing gas evaluated at the average pressure, p_a is the reference pressure at which the volumetric flow rate q_a was measured, L and A are the length and cross-sectional area of the specimen, and p_1 and p_2 are the upstream and downstream pressures. At a particular pressure gradient, it is mainly the permeability that determines the gas flow rate through the core. For cores with ultra low permeability, it is hard to measure accurately the gas flow rate. The permeability of such samples is measured using a transient method in which the differential pressure between upstream and downstream vessels across a sample is monitored (Pan 2010). The permeability is calculated based on the following equations:

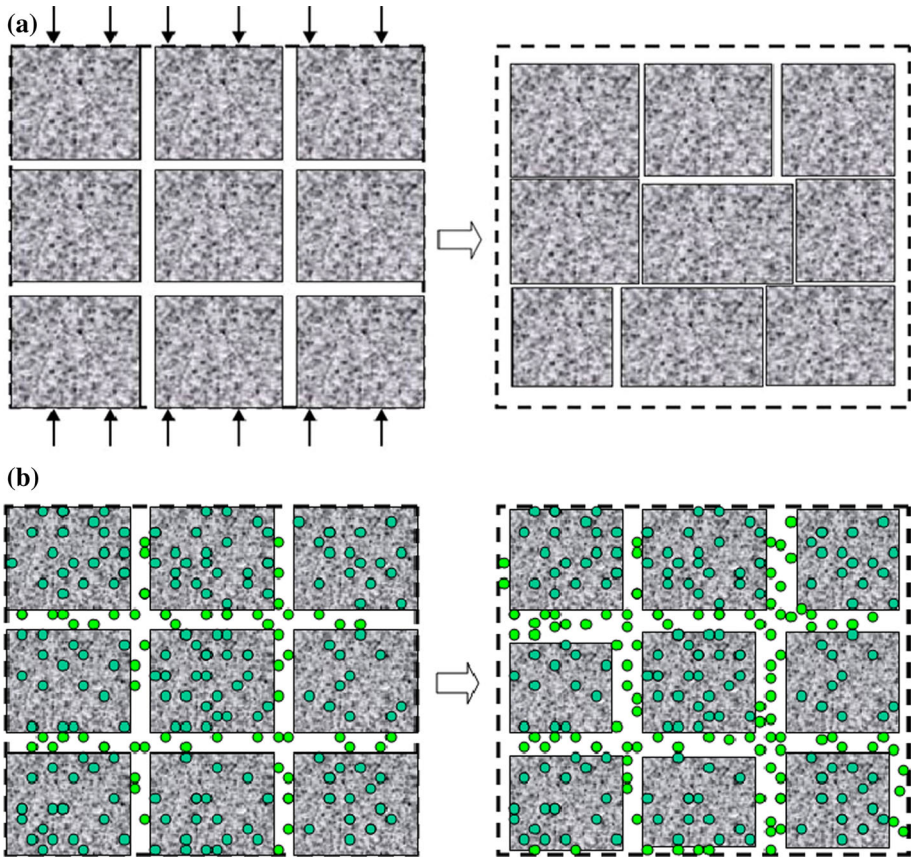


Fig. 2 Mechanisms of permeability change of coal **(a)** Cleft closure and permeability decrease due to increase of effective stress. **(b)** Matrix shrinkage and permeability increase due to gas desorption

$$\frac{p_u - p_d}{p_{u,0} - p_{d,0}} = e^{\alpha t}, \tag{2}$$

where $p_{u,0} - p_{d,0}$ is the initial upstream and downstream pressure difference, $p_u - p_d$ is the upstream and downstream pressure difference at time t , and

$$\alpha = \frac{k}{\mu_g C_g L^2} V_R \left(\frac{1}{V_u} + \frac{1}{V_d} \right), \tag{3}$$

where k is the permeability of the sample, μ_g and C_g are the viscosity and compressibility of the test gas, L and V_R are the sample length and volume, and V_u and V_d are the volume of upstream and downstream vessels.

The amount of adsorption is measured based on material balance using either a volumetric or gravimetric method (Jessen et al. 2008; Harpalani and McPherson 1986; Hall et al. 1994). For volumetric methods, solid (adsorbent) is placed in a vessel of known volume that is connected with a charging vessel of known volume. The whole system is first evacuated. Then the valve between the two vessels is closed, and gas (adsorbate) is filled into the charging vessel. The gas pressure in the charging vessel is read before the valve between the two vessels is opened and gas is allowed to flow into the adsorbent vessel and

contact with the solid. The pressure of the whole system is read when it reaches equilibrium. The initial moles of adsorbate in the charging vessel are calculated based on the volume of the charging vessel and the initial gas pressure. The moles of adsorbate in the gaseous phase at equilibrium are calculated based on the dead volume of the system (volume of the system minus the volume of the adsorbent) and the equilibrium pressure. The difference between the moles of adsorbate at the initial and equilibrium condition is the moles adsorbed. Gravimetric methods measure the weight change of the adsorbent when exposed to the adsorbate gas at a specific pressure and temperature. Solid (adsorbent) is placed at one side of a high accuracy balance in a pre-evacuated system. Gas is then allowed into the system. The weight change of the solid is captured by the balance. The weight change at pressure equilibrium is considered as the weight of the adsorbed adsorbate.

Strain is calculated based on measurement of the amount of deformation in the length or volume of the specimens. Axial and radial strains are measured using strain gages (Harpalani and Zhao 1989; Pan 2010). Volumetric strain is calculated as (Pan 2010)

$$\varepsilon_V = \varepsilon_{r1} + \varepsilon_{r2} + \varepsilon_a, \quad (4)$$

where ε_V is the volumetric strain, ε_{r1} and ε_{r2} are the radial strains measured in two perpendicular directions, and ε_a is the axial strain.

In our study, the amount of adsorption and the composition of the adsorbed phase (for binary mixtures) was calculated based on measurements using a volumetric method. The sorption-induced volumetric strain was obtained by monitoring the volume of the core with adsorption. And permeability was calculated using the Darcy equation for gas flow based on coreflood tests.

3 Experimental Specimens, Apparatus, and Procedures

In a previous study, we measured the permeability of a ground coal pack using methane, nitrogen, carbon dioxide, and several binary mixtures of nitrogen and carbon dioxide at increasing pore pressures (from 350 to about 7,000 kPa) and constant effective confining pressure (2,758 kPa) at room temperature. Results showed that for a given test gas, the permeability of coal decreased as the pore pressure increased. The magnitude of the permeability reduction was dependent on the pressure and composition of the test gas. Pure carbon dioxide caused the most significant permeability reduction, followed by methane and then nitrogen. In the case of CO₂& N₂ binary mixtures, the more carbon dioxide (by mole fraction) in the test gas, the severer the permeability reduction. The permeability reduction was believed to be mainly caused by sorption-induced swelling of the coal, given the fact that the effective confining pressure was kept constant.

The purpose of the current study was to measure simultaneously gas adsorption, the associated volumetric change, and permeability change to gain insight on the correlation between gas adsorption on coal and the sorption-induced volume and permeability change of coal. The novel aspects of this study are as follows:

1. Adsorption, sorption-induced strain, and permeability were measured on the same piece of core with the same apparatus. The measurements of adsorption and sorption-induced strain were simultaneous. Permeability was measured before and after adsorption on the same core.
2. Cored coal plugs, instead of ground coal pack, were used. The intact coal plugs preserved some of the small scale cleats presented in real coalbed methane reservoirs. Several coal

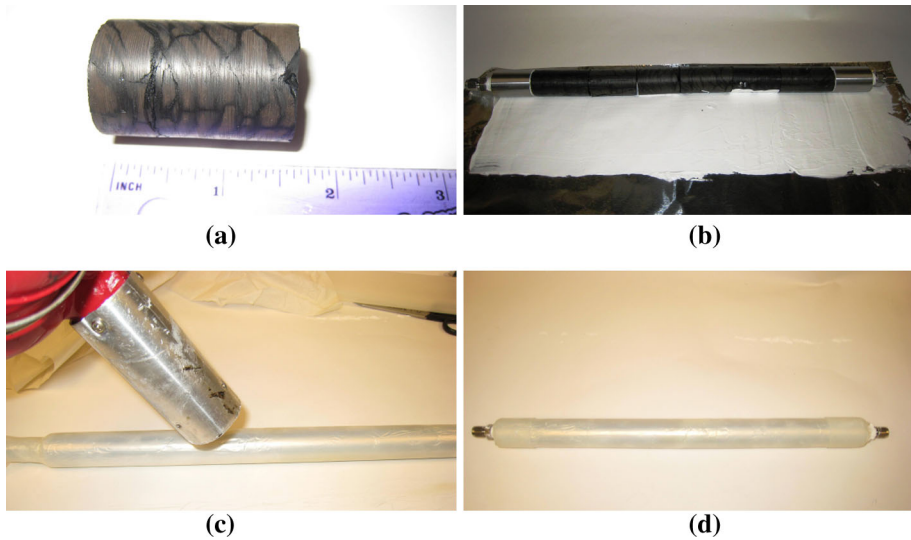


Fig. 3 Composite core used in the experiments (a) A piece of coal plug. (b) Assembled coal plugs. (c) Heating the shrinkable tube. (d) The composite core

plugs were assembled together to make a composite core. The larger sample volume delivers more moles of total adsorption, thus smaller relative error in the measurements.

- Several binary mixtures of CO_2 and N_2 were used in addition to pure gases. Gas chromatography was used to measure the initial and equilibrium gas compositions, thus a direct calculation of the composition of the adsorbed phase.

3.1 Test Samples

The coal samples used in the current study were collected at a mine face of the Wyodak-Anderson coal zone, Powder River Basin, Montana. As collected, the samples were in big chunks, Fig. 1. The samples were heavily wrapped with plastic bubble wrap and air transported to the laboratory in wood boxes. Upon receipt, the samples were unpacked, thoroughly washed using distilled water, and then kept immersed in deaerated distilled water to avoid further oxidization of the coal surfaces.

Cylindrical specimens were cored from the big chunks using a thin-wall diamond core bit with inner diameter of 1 inch. Water was used as a cooling agent. Core recovery was generally poor due to the brittle nature of the coal. The length of the retrieved specimens varied from less than 1 inch to about 3 inches. Fractures were clearly observable in all of the specimens, Fig. 3a. The end faces of the specimens were polished flat using sandpaper. After washing off any fines on the surfaces, several pieces of the specimens were aligned to form a composite core. Two stainless steel end plugs with holes as gas inlet and outlet were placed at the two ends of the composite core. The whole piece (the composite core and the end plugs) was wrapped with aluminum foil that was coated with silica gel, Fig. 3b. The gel was used to make sure no flow path formed around the core in the axial direction. The aluminum foil was used to prevent gas diffusion to the confining fluid while still allowing for inspection of the core by computed tomography (CT) scanning. The composite core was then placed in a piece of Teflon heat shrink tubing.

Fig. 4 Viton and Teflon tubes after 2 days in contact with water and CO₂ under pressure



Teflon was chosen among other materials after running several simple tests to confirm it did not degrade in the presence of water and carbon dioxide. Figure 4 shows pictures of several Teflon and Viton tubes after being in a sealed container filled with some water and CO₂ gas for 2 days. The container pressure was around 2,000 kPa. Teflon did not show any degradation.

A heating gun was used to heat shrink the tubing tightly onto the core, Fig. 3c and d. The core was then placed under heating lamps (60 °C) and evacuated using a vacuum pump for a few days to make sure that all the moisture and gas contents in the core were removed. The evacuated core was placed inside an aluminum confining pressure sleeve with floating heads at the two ends. Stainless steel tubing connected with the inlet and outlet of the end plugs of the core went through the floating heads of the confining sleeve. The whole coreholder was readily connected with the rest of the apparatus.

As a pre-screening process, permeability of the core was measured using helium. A good core for our study required sufficient lateral permeability to allow gas flow at a measurable rate with no direct flow bypass along the lateral side of the core. Only the well-consolidated coals were successfully cored. Therefore, the permeability of the composite core was expected to be lower than the actual coal seam. Two composite cores were made and discarded before a third one, that fulfilled the permeability requirements, was obtained. The final core consisted of eight specimens and had a total length of 27.6 cm. The average wet density of the coal was measured to be 1.21 g/cm³.

The core was scanned using a CT scanner when it was first assembled, after being evacuated under heat, and after confining pressure was applied. The CT images of several cross-sections of the core are shown in Fig. 5. Low CT numbers indicate low density. Fractures in the core were also observable from the CT images. The dry coal has lower density compared with when it was wet. When confining pressure was applied, the core was compressed and some of the fractures were closed.

3.2 Apparatus and Initial Measurements

An experimental apparatus capable of conducting all three measurements, sorption, volumetric strain, and permeability, on the same piece of core was designed, as shown in Fig. 6. The major components of the apparatus were the hydrostatic coreholder, three precision high pressure syringe pumps connected to a PC and run in either constant pressure or constant flow rate mode, two piston accumulators each of which consists two compartments separated by a

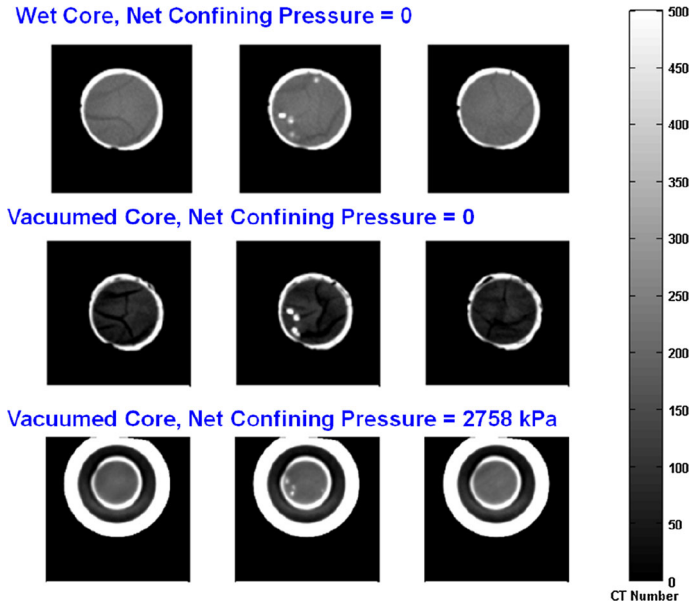


Fig. 5 CT images of the composite core before experiments at different conditions. Inlet to outlet from *left to right*. Raw CT numbers are shown (Low CT numbers indicate low density. Fractures are indicated by the *darkest areas*). The *white ring* around the core is the layer of silicon gel, the *second ring* in the images in the third row shows the stainless confining vessel

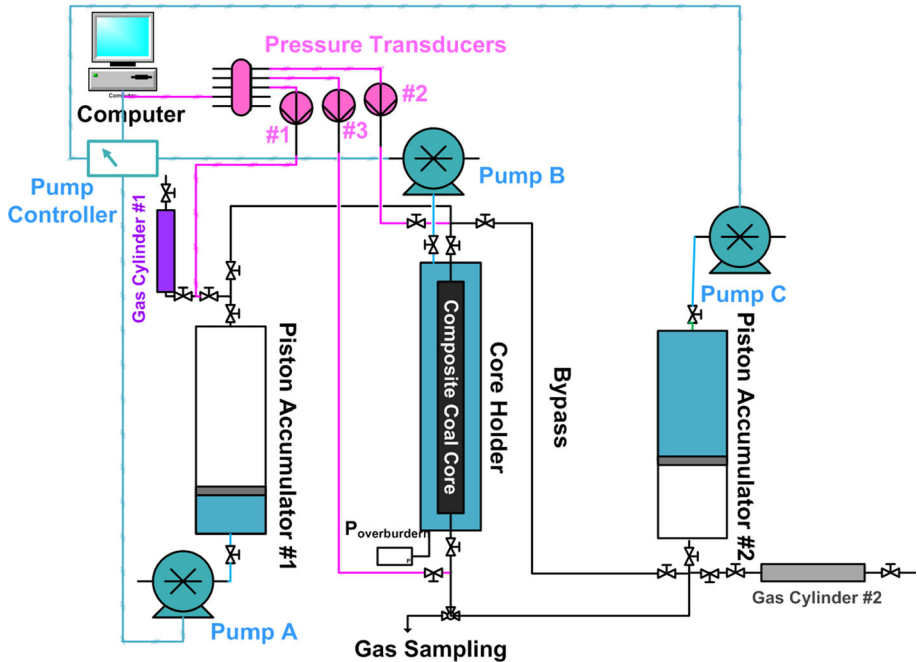


Fig. 6 Schematic of experimental apparatus for measurement of adsorption, strain, and permeability

piston, three pressure transducers wired to a data acquisition device that was also connected with the PC, and two gas cylinders for the supply of gas. Labview software was used to monitor and record the pressure, flow rate, and volume of the precision high pressure pumps.

After assembly, the whole apparatus was first evacuated using a vacuum pump. The dead volumes of each compartment (space separated by every two valves) within the system were determined using helium based on a gas expansion method. The pore volume of the core was thus obtained. The total volume of the core was calculated based on the cross-sectional area and length of the core. The initial porosity of the core was calculated to be 12%. The dry weight of the core was estimated to be 151.77 g based on the wet weight and pore volume of the core and the density of water. At the end of dead volume measurement, the valves at the two ends of the coreholder and the bypass line were closed. The system was separated into two compartments at the two sides of the core. A pressure difference of 140 kPa was established between the two compartments by setting the pressures of the two pumps connected with the piston accumulators. The valves to the core were then opened and helium was allowed to flow through the core while the pressure gradient decayed. The upstream and downstream pressures and the gas flow rates were captured by the pumps and recorded. Permeabilities were then calculated using Eq. (1). The average helium permeability of the core was 18 *md* at pore pressure of 450 kPa and confining pressure of 3,210 kPa. Coal beds usually have permeability ranging from 0.1 to 30 *md* (McKee et al. 1988). The permeability of the core is within the range of the permeability of typical coalbed methane reservoirs.

Sorption, volumetric strain, and permeability measurements were conducted using the following gases in the order listed: 50% CO₂ & 50% N₂ (mole fraction) binary gas mixture, pure CO₂, pure N₂, pure helium, and 75% CO₂ & 25% N₂ binary gas mixture. For the pure gases, bottled gases from commercial manufacturers with 99.0% purity were used. The binary mixtures of CO₂ and N₂ were made in the laboratory.

3.3 Sorption Measurement

A volumetric method was used for adsorption measurement. Prior to adsorption measurement with each gas, the whole system was evacuated using the vacuum pump for a few days to make sure that all the moisture and gas contents in the core and other parts of the system were removed. Then the valves leading to the core were closed, and gas was charged into the system. The adsorption pressure was set using the pumps connected with the piston accumulators. The confining pressure was adjusted to maintain about 2,800 kPa net effective stress on the coal for all measurements. Figure 7 shows the adsorption cell. To start the adsorption process, the valves leading to the coreholder were opened to let the gas flow inside. Pressure within the adsorption cell was monitored by the pressure transducers. Adsorption equilibrium was considered to be reached when the pressure within the adsorption cell stabilized.

The total amount of adsorption was calculated based on the dead volume of the adsorption cell and the initial and equilibrium pressures of the system:

$$n_{t,ads} = \frac{1}{RT} \left(\frac{p_i V_{DV,1}}{Z_i} - \frac{p_e V_{DV,t}}{Z_e} \right), \quad (5)$$

where R is the universal gas constant, T is the experimental temperature (22 °C), p_i and p_e are the initial and equilibrium pressures, $V_{DV,1}$ and $V_{DV,t}$ are the dead volumes of corresponding compartments measured using helium, Z_i and Z_e are the compressibility factor (function of the temperature, pressure, and gas composition) of the gas prior to adsorption and after equilibrium being reached. The compressibility factors for gas were obtained by conducting

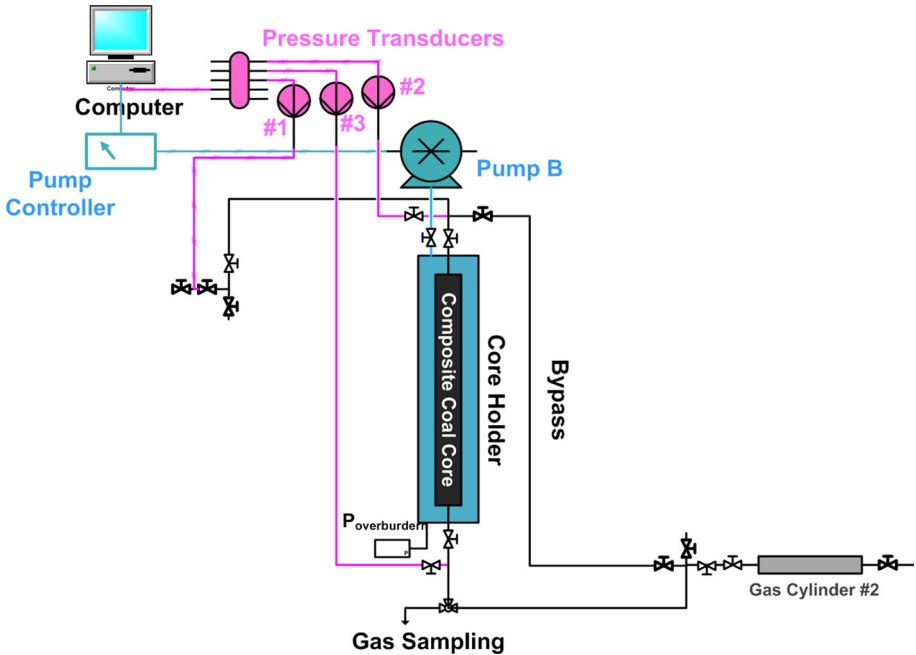


Fig. 7 The adsorption cell (valves in *bold* were closed while the adsorption measurement)

flash calculations at the experimental temperature and pressure based on the Peng-Robinson equation of state (Reid et al. 1987).

For binary adsorption, after the system reached adsorption equilibrium, the valves leading to the coreholder were closed, then a sample of the equilibrium gas was collected from the adsorption cell. The gas samples were analyzed afterward using gas chromatography. The amount of adsorption for each component was calculated based on material balance:

$$n_{i,ads} = \frac{1}{RT} \left(\frac{p_i V_{DV,1} y_i}{Z_i} - \frac{p_e V_{DV,t} y_e}{Z_e} \right), \tag{6}$$

where y_i and y_e are the initial and equilibrium gas phase compositions. The adsorbed phase composition was calculated as

$$x_i = \frac{n_{i,ads}}{n_{t,ads}} \tag{7}$$

Equation (5) does not take into account of the volume occupied by the adsorbed phase. The value obtained using Eq. (5) is called the measured adsorption or Apparent Gibbs Adsorption (Hall et al. 1994). Taking into account of the volume of the adsorbed phase, the absolute adsorption was calculated as

$$n_{ads,absolute} = \frac{n_{ads,measured}}{1 - \frac{v_{ads}}{v_{gas}}}, \tag{8}$$

where v_{ads} and v_{gas} are the molar volume of the adsorbed and gas phases. The molar volume of the adsorbed phase was assumed to be equal to the stacking volume of one mole of adsorbate molecules (Hall et al. 1994). According to the Peng–Robinson equation of state (Reid et al.

1987), the molar volume of the adsorbed phase is

$$v_{\text{ads},i} = \frac{0.0778RT_{c,i}}{p_{c,i}}, \quad (9)$$

where $T_{c,i}$ and $p_{c,i}$ are the critical temperature and pressure of component i . The calculated molar volumes of N_2 and CO_2 are, respectively, $24.081 \text{ cm}^3/\text{mol}$ and $26.655 \text{ cm}^3/\text{mol}$. The molar volume of component i in the gas phase was calculated based on the real gas law:

$$v_{\text{gas},i} = \frac{Z_e RT}{p_e} \quad (10)$$

The molar volume of mixtures was calculated as the molar percentage weighted average of the individual component molar volume.

3.4 Volumetric Strain Measurement

The confining pressure pump was in constant pressure mode for measurements at each pressure. The liquid volume in the pump was recorded during the sorption measurement. The change of the pump volume was a direct indication of the change of the core volume. The volumetric strain was calculated using the following equation:

$$\varepsilon_{\text{ads}} = \frac{\Delta V_{\text{core}}}{V_{\text{core},i}}, \quad (11)$$

where ΔV_{core} is the volume change of the core, and $V_{\text{core},i}$ is the initial volume of the core prior to adsorption.

3.5 Permeability Measurement

Following the adsorption and volumetric strain measurements, permeability of the core was measured at the adsorption equilibrium pressure as described in Sect. 3.2. A pressure difference of 140 kPa was set at the two sides of the core. Caution was taken to make sure that the average pressure equaled to the equilibrium adsorption pressure such that no additional adsorption/desorption occurred during the permeability measurement. The valves leading to the coreholder were then opened to allow gas flow through while the pressure gradient decayed. The upstream and downstream pressure and the flow rates were captured and recorded by the pumps connected with the piston accumulators. Permeability was calculated using Eq. (1). Figure 8 shows the pressure readings at the inlet and outlet of the core and the calculated permeability after adsorption of a binary mixture of 75 % CO_2 & 25 % N_2 at 2,668 kPa. An average permeability of 1.12 md was obtained based on the data at 1.6–3.2 h time interval.

After the permeability measurement, the valves at the two ends of the coreholder were closed and the valves at the two ends of the bypass line were opened. The system pressure was set to a new value using the pumps connected with the piston accumulators. The confining pressure was adjusted accordingly to make sure that the effective confining pressure was the same. Measurements of adsorption, volumetric strain, and permeability were repeated at the new pressure. For each test gas, measurements at 5–7 pressure points were conducted up to 6,000 kPa. The system pressure was then decreased step by step, and the amount of desorption and permeability was measured again.

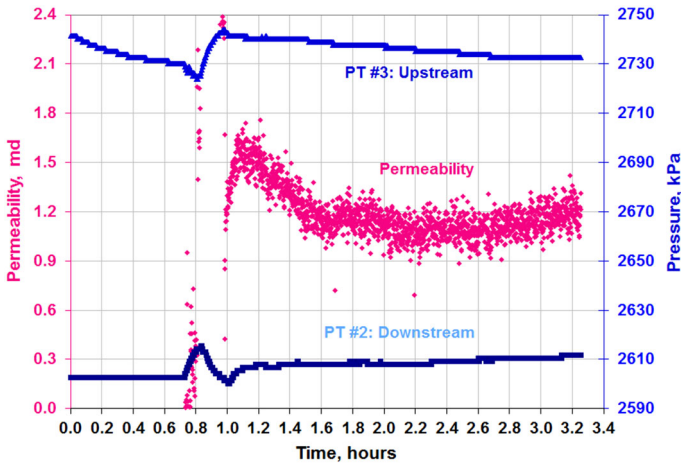


Fig. 8 Permeability measurement after adsorption of binary mixture of 75%CO₂/25%N₂ at 2668 kPa (uncalibrated), confining pressure = 5,592 kPa

Table 1 Adsorption of pure CO₂, experiment temperature = 22 °C

Equilibrium Pressure (kPa)	Effective Confining Pressure (kPa)	$n_{t,ads}$ Experimental (mol/kg)	Z_{equil}	$v_{gas, equ}$ (cm ³ /mol)	$n_{t,ads}$ Absolute (mol/kg)
0		0			0
168.55	2,934.09	0.5782	0.9905	1,4421.01	0.5793
422.75	2,886.73	0.7667	0.9759	5,664.99	0.7703
685.82	2,899.45	0.9568	0.9605	3,436.88	0.9643
1,095.32	2,903.64	1.1567	0.9361	2,097.28	1.1716
1,564.41	2,917.18	1.3706	0.9073	1,423.24	1.3968
2,075.98	2,888.25	1.5763	0.8746	1033.87	1.6180
2,620.50	2,895.30	1.7998	0.8381	784.85	1.8631
3,597.98	2,952.04	2.1811	0.7667	522.93	2.2982
4,603.99	2,980.24	2.5920	0.6811	363.04	2.7974
5,317.77	2,955.94	2.8518	0.6061	279.70	3.1522
4,945.67	3,121.20	2.6576	0.6473	321.19	2.8981
3,745.69	3,149.07	2.1974	0.7551	494.71	2.3226
2,415.12	3,100.69	1.7078	0.8521	865.82	1.7620
1,099.13	3,382.47	1.1482	0.9359	2089.58	1.1631

4 Experimental Results

The experimental-adsorption/desorption data are tabulated in Tables 1, 2, 3 and 4 and plotted in Fig. 9. Obviously, the amount of adsorption increased with the increase of pressure, and decreased with the decrease of pressure. As shown in Fig. 9, no obvious adsorption/desorption hysteresis was observed. At the same pore pressure, the amount of adsorption for CO₂ was greater than that of N₂. The greater the fraction of CO₂ in the injection gas, the greater the total

Table 2 Adsorption of pure N₂, experiment temperature = 22 °C

Equilibrium Pressure (kPa)	Effective Confining Pressure (kPa)	$n_{t,ads}$ Experimental (mol/kg)	Z_{equil}	$v_{gas,equ}$ (cm ³ /mol)	$n_{t,ads}$ Absolute (mol/kg)
0		0			0
602.15	2,845.23	0.0934	0.9973	4,091.70	0.0940
1,188.51	2,810.45	0.1386	0.9948	2,067.83	0.1404
1,997.37	2,828.96	0.1830	0.9919	1,226.85	0.1871
3,019.86	2,840.68	0.2331	0.9888	808.91	0.2411
4,055.66	2,839.09	0.2656	0.9864	600.86	0.2780
5,410.95	2,862.75	0.3072	0.9844	449.45	0.3267
6,199.53	2,763.65	0.3114	0.9838	392.04	0.3343
5,270.86	3,002.85	0.2901	0.9846	461.49	0.3080
4,233.79	3,005.70	0.2456	0.9861	575.40	0.2576
3,192.92	3,012.36	0.1934	0.9884	764.76	0.2004
2,165.36	3,005.71	0.1275	0.9913	1130.98	0.1306
823.38	2,968.73	0.0227	0.9963	2,989.30	0.0229

Table 3 Adsorption of 50%CO₂&50%N₂ binary mixture, experiment temperature = 22 °C

Equilibrium Pressure (kPa)	Effective Confining Pressure (kPa)	$n_{t,ads}$ Absolute (mol/kg)	x_{CO_2}	y_{CO_2}	S_{CO_2,N_2}
0		0	0	0	0
512.96	2,934.42	0.2598	0.7244	0.4967	2.6632
803.09	2,851.13	0.3453	0.7195	0.4810	2.7670
1,183.43	2,815.52	0.4266	0.6955	0.4752	2.5233
1,660.13	2,821.46	0.5135	0.6520	0.4715	2.1004
2,354.26	2,816.81	0.5461	0.5985	0.4712	1.6727
3,073.74	2,786.80	0.5754	0.5686	0.4653	1.5148
3,738.71	2,811.31	0.6335	0.5681	0.4568	1.5638
4,775.14	2,809.09	0.6813	0.5650	0.4425	1.6364
5,927.58	2,918.39	0.8536	0.5392	0.4321	1.5376

amount of adsorption. The separation factor between two components of multicomponent adsorption is defined as (Yang 1987)

$$S_{i,j} = \frac{x_i/y_i}{x_j/y_j}. \quad (12)$$

Separation factors of CO₂ to N₂ were greater than one, but still in the order of one. The separation factors obtained in this study were smaller than those obtained by Hall et al. for supercritical CO₂ & N₂ adsorption on their wet ground coal samples (Hall et al. 1994). The separation factors obtained by Hall et al. and in this study both decreased with the increase of pressure.

Table 4 Adsorption of 75%CO₂&25%N₂ binary mixture, experiment temperature = 22 °C

Equilibrium Pressure (kPa)	Effective Confining Pressure (kPa)	$n_{t,ads}$ Absolute (mol/kg)	x_{CO_2}	y_{CO_2}	S_{CO_2,N_2}
0		0.0000			
483.05	2,964.33	0.4545	0.8700	0.7221	2.5754
941.28	2,850.83	0.6003	0.8506	0.7340	2.0632
1,310.16	2,826.70	0.7212	0.8332	0.7417	1.7396
1,654.31	2,827.28	0.8193	0.8184	0.7457	1.5366
1,999.10	2,827.23	0.9021	0.8132	0.7544	1.4169
2,670.29	2,845.51	1.0471	0.8058	0.7565	1.3353
3,664.73	2,885.29	1.1603	0.8135	0.7818	1.2168
3,622.26	2,789.86	1.1038	0.8123	0.7792	1.2261
2,776.22	2,946.43	1.0141	0.8111	0.7678	1.2984
2,155.65	2,980.95	0.9053	0.8099	0.7779	1.2159
1513.60	2,967.99	0.7397	0.8087	0.7757	1.2221
893.75	2,967.32	0.4934	0.8075	0.7741	1.2239
508.40	2,973.46	0.2821	0.8063	0.7788	1.1821

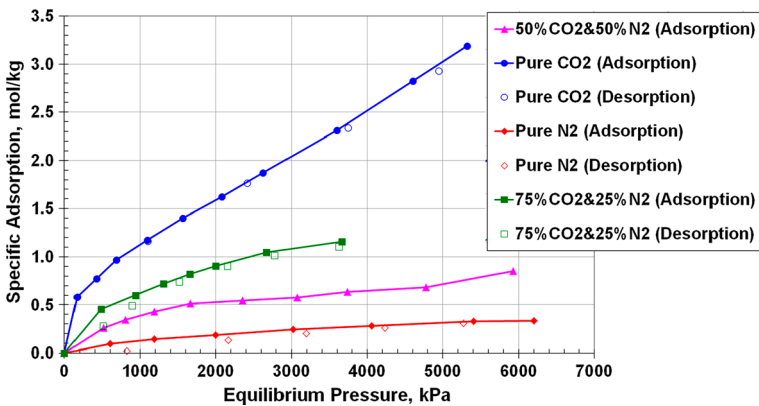


Fig. 9 Specific adsorption versus pressure. Closed symbols represent adsorption experimental data, and open symbols represent desorption experimental data

Figure 10 shows volumetric strain with the injection of different gases at escalating pressures. Compared with the results of Hagin and Zoback (2010), our volumetric strain values might be greater. The volumetric strain with the injection of CO₂ obtained by Hagin and Zoback was less than 1 % at a pore pressure of 1000 kPa and effective pressure of 5,000 kPa. The volumetric strain with the injection of CO₂ at 1,000 kPa was almost 2 % under an effective pressure of 2,800 kPa for our system.

Figure 11 plots the permeability of the core after adsorption of different gases versus pore pressure. The permeabilities at zero pressure are actually the helium permeability of the core prior to the injection of the specific gas. The helium permeability of the core decreased in the process of the experiments indicating that the sorption-induced permeability reduction was

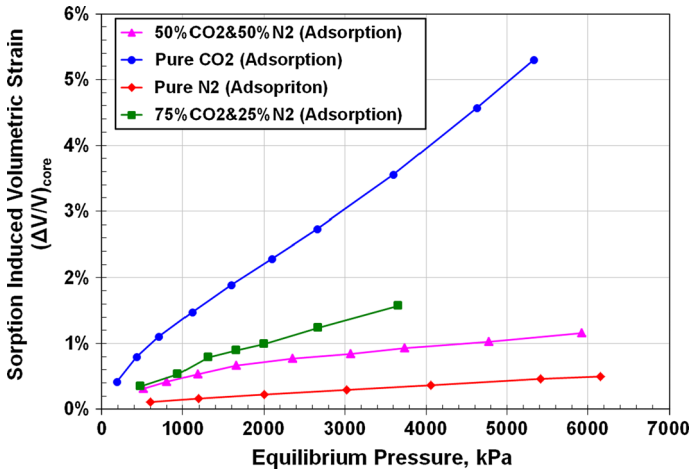


Fig. 10 Sorption-induced volumetric strain versus pressures. Symbols represent the experimental data

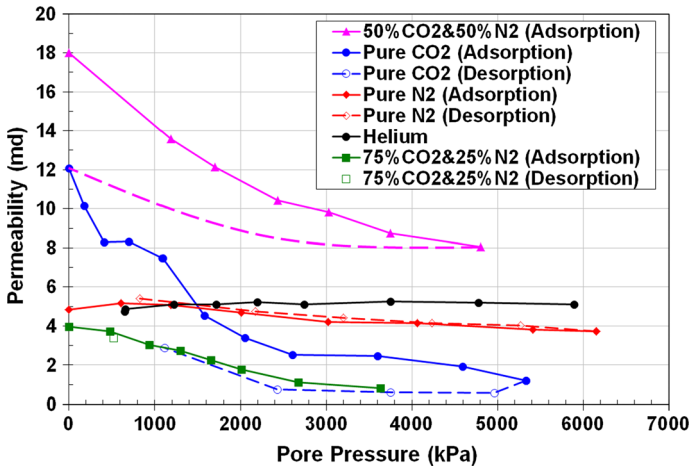


Fig. 11 Permeability of the core with adsorption and desorption of different gases. Closed symbols represent experimental results with gas adsorption, and open symbols represent experimental results with gas desorption. Note Permeability of the core was not measured during desorption of 50 %CO₂&50 %N₂. The dashed pink line shows one possible path for the permeability change with desorption

not fully reversible. One possible explanation for that is sorption (or sorption-induced strain) causes permanent mechanical damage to the coal. To compare the magnitude of permeability reduction for different injection gases, permeability reduction was calculated

$$R_k = \frac{k}{k_0}, \tag{13}$$

where k_0 is the helium permeability of the core prior to the adsorption of a specific gas, and k is the permeability of the core after adsorption of the gas at pressure p . Permeability reduction less than unity indicates permeability decreases. Permeability reduction is plotted in Fig. 12. It is observed that

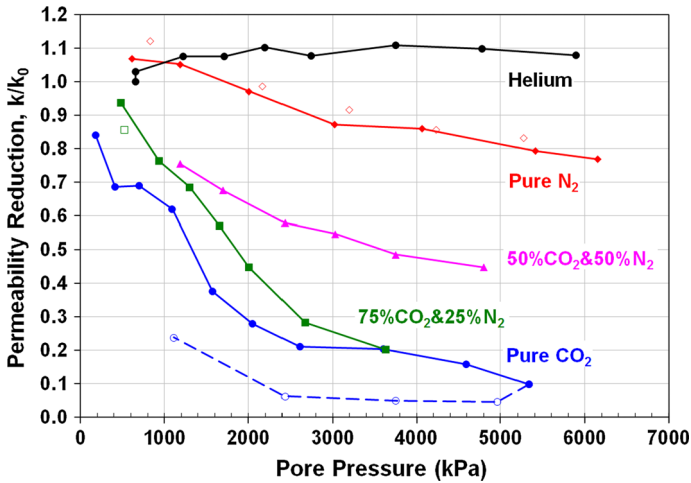


Fig. 12 Permeability reduction of the core with adsorption and desorption of different gases. *Closed symbols* represent experimental results with gas adsorption, and *open symbols* represent experimental results with gas desorption

1. Under constant effective stress, the permeability of the core decreases with the adsorption of CO_2 , N_2 , or a binary mixture of the two at escalating pore pressure.
2. The most severe permeability reduction occurred with pure CO_2 adsorption. The permeability of the core after adsorption of CO_2 at 5300 kPa became one tenth of the value prior to adsorption. For binary mixtures, the greater the partial pressure of CO_2 in the injection gas, the more severe the permeability reduction.
3. Permeability of the core rebounded when the pore pressure decreased under constant effective stress. It did not, however, recover to the permeability value prior to adsorption. This might partly due to hysteresis with gas adsorption. Besides that, the core might go through irreversible physical change (crushing) in the process of the experiments.
4. Under constant effective stress, helium permeability of the core only increased slightly with the increase of pore pressure. The Klinkenberg effect was negligible as documented next.

Klinkenberg Effect

Besides effective stress and sorption, pore pressure may also affect the gas permeability of low-permeability rocks through the “Klinkenberg effect” (Klinkenberg 1941; Tanikawa and Shimamoto 2006):

$$k = k_0 \left(1 + \frac{b}{p_m} \right), \quad (14)$$

where k_0 is the permeability to liquid or gas at infinite pressure, p_m is the mean gas pressure, and b is the Klinkenberg slip factor.

The average distance traveled by a molecule between successive collisions with the other molecules is called the *mean free path*. The Klinkenberg effect occurs when the dimension of the mean free path of the gas is of the same magnitude as that of the flow path. At this circumstance, the gas molecules have appreciable interaction (i.e., collision) with the flow path surface, which contributes to an additional flow component besides the Darcian flow, thus higher permeability. The mean free path of a gas is (Bird et al. 1960)

$$\lambda = \frac{1}{\sqrt{2}\pi d^2 \bar{N}}, \quad (15)$$

where λ is the mean free path, d is the molecular diameter, and \bar{N} is the number of molecules per unit volume. The kinetic diameters of the molecules of N_2 and CO_2 are 3.64 Å and 3.3 Å, respectively (Adamson and Gast 1997). Based on the real gas law,

$$\bar{N} = N_A \frac{n}{V} = N_A \frac{p}{ZRT}, \quad (16)$$

where $N_A = 6.02 \times 10^{23}$, is the Avogadro constant. The values of the mean free path of N_2 and CO_2 calculated based on Eq. (15) and (16) are in the magnitude of several to tens of nanometers over the pressure ranges of interest (1,000–5,000 kPa). The mean free path of helium is even smaller than those of N_2 and CO_2 .

The dimension of the flow path in porous media is estimated using the Carmen–Kozeny (Lake 1989):

$$D_p = \sqrt{\frac{72\tau(1-\phi)^2 k}{\phi^3}}, \quad (17)$$

where D_p is the pore (flow path) size, τ is the tortuosity that is usually between 2 and 5 for reservoir rocks of interest (Lake 1989), ϕ is the porosity, and k is the permeability. The diameters of the flow paths in typical coalbed methane reservoirs (greater than 1 md) are estimated to be in the magnitude of several micrometers, which is several magnitude larger than the mean free path of N_2 , CO_2 , and Helium. Gas slippage seems to be of minor consequence low rank coal with moderate permeability (greater than 1 md). It may be a concern for coal with lower permeability.

5 Summary

Gas adsorption and desorption on coal, and the consequent volumetric and permeability changes of the coal were measured on a composite core at varying pore pressures and constant effective confining pressure and temperature. Pure CO_2 and N_2 , CO_2 & N_2 binary mixtures, and helium were used as test gases. The total amount of sorption was measured based on a volumetric method and material balance. The initial and equilibrium gas phase compositions were measured, and the composition of the adsorbed phase was calculated based on the material balance. Sorption-induced volumetric strain was obtained by monitoring the volumetric change of the core through the confining pressure pump. Permeability was measured based on Darcy flow of gas. Experimental results showed that

1. At constant temperature, the amount of gas adsorption on coal increased with the increase of pressure, and decreased with the decrease of pressure. No obvious adsorption/desorption hysteresis was observed. At the same pore pressure, the amount of adsorption for CO_2 was about eight times of that of N_2 . For CO_2 & N_2 mixtures, the greater the fraction of CO_2 in the gas, the greater the total amount of adsorption. The separation factors of CO_2 to N_2 were less than 3 for the pressures and gas compositions we tested. With the increase of pressure, the separation factor decreased.
2. Under constant effective stress, the volume of the core increased with the increase of pore pressure. Comparing Figs. 9 and 10, it appeared that the volumetric strain had a direct correlation with the amount of adsorption. The largest volumetric strain was measured when CO_2 was injected, the volume of the core increased more than 5 % at 5318 kPa.

3. Under constant effective stress, the permeability of the core decreased with the increase of pore pressure. The more CO₂ in the gas, the greater the permeability reduction. After adsorption of CO₂ at 5270 *kPa*, the permeability of the core was only one tenth of the value before adsorption. Permeability of the core rebounded when the pore pressure was decreased. It did not, however, recover to the permeability value prior to adsorption even after several days of evacuation. The Klinkenberg effect was not obvious in the core we tested.

The main contribution of this work is that it presented a new experimental setup that enabled simultaneous and consequent measurements of gas adsorption&desorption on coal, and the sorption-induced volumetric strain and permeability change of the coal on the same piece of core. Simultaneous measurement of the volumetric change of the core with adsorption was possible by using heat shrinkable tube as the core holder and maintaining the confining pressure using a high accuracy syringe pump running in constant pressure mode. The apparatus is readily modified to measure permeability based on transient flow to accommodate cores with lower permeability. Keeping constant pore pressure while changing the confining pressure, the effect of effective stress on permeability can also be tested using the same apparatus. The apparatus can be setup on a movable bench, such that it can be moved to a CT scanner to acquire CT images before and after adsorption. CT images may reveal some physical changes of the core caused by gas adsorption and desorption. That will also help to understand the mechanisms of the permeability change.

There are several limitations of the experimental setup. First, only well-consolidated samples are cored successfully. In real coal seams where larger fractures may present, the magnitude of permeability change may be smaller. Using cores of larger diameters can preserve some larger fractures and be used to test the effect of matrix&fracture dimensions. Secondly, the system has lots of connections that must be checked for leaks. It is critical to make sure that there is no leakage in the whole process of the experiments. Given the small amount of adsorption for certain test gases, leakage badly affects the accuracy of the experimental data.

Acknowledgments This paper was prepared with the support of the Global Climate and Energy Project (GCEP). This support is gratefully acknowledged. However, any opinions, findings, conclusions, or recommendations expressed herein are those of the author and do not necessarily reflect the views of GCEP and its supporters.

References

- Adamson, A.W., Gast, A.P.: *Physical Chemistry of Surfaces*, 6th edn. Wiley, New York (1997)
- Ares, Y., Barron, K.: The effect of gas sorption on the strength of coal. *Mining Sci. Technol.* **6**, 291–300 (1998)
- Bird, R. B., Stewart, W. E., and Lightfoot, E. N.: *Transport Phenomena*, Wiley, ISBN: 0 471 07392 X (1960)
- Gray, I.: Reservoir engineering in coal seams: part 1—the physical process of gas storage and movement in coal seams. *SPE Reserv. Eng.* **2**(1), 28–34 (1987)
- Hagin, P., Zoback, M. D.: Laboratory studies of the compressibility and permeability of low-rank coal samples from the Powder River Basin, Wyoming, USA, Paper 10–170, 44th U.S. rock mechanics symposium and 5th U.S.—Canada rock mechanics symposium, Salt Lake City, Utah, 27–30 June 2010
- Hall, F.E., Zhou, C. H., Gasem, K.A.M., Robinson, R. L., Jr., Yee, D.: Adsorption of pure methane, nitrogen, and carbon dioxide and their binary mixtures on wet fruitland coal. Paper SPE 29194 presented at eastern regional conference and exhibition held at Charleston, WV, U.S.A. 8–10 Nov 1994
- Harpalani, S., Zhao, X.: The unusual response of coal permeability to varying gas pressure and effective stress. In: *The 30th U.S. symposium on rock mechanics (USRMS)*, Morgantown, WV, 19–22 June 1989
- Harpalani, S., McPherson, M.J.: Retention and release of methane in underground coal working. *Geotech. Geol. Eng.* **4**, 217–233 (1986)

- Jahediesfanjani, H., Civan, F.: Damage tolerance of well-completion and stimulation techniques in coalbed methane reservoirs. *J. Energy Res. Technol.* **127**(3), 248–256 (2005)
- Jessen, K., Tang, G.-Q., Kovscek, A.R.: Laboratory and simulation investigation of enhanced coalbed methane recovery by gas injection. *Transp. Porous Media* **73**(2), 141–159 (2008). doi:[10.1007/s11242-007-9165-9](https://doi.org/10.1007/s11242-007-9165-9)
- Katz, D.L.V., Lee, R.L.: *Natural Gas Engineering: Production and Storage*. McGraw-Hill, New York (1990)
- Klinkenberg, L.J.: *The Permeability of Porous Media to Liquids and Gases, Drilling and Production Practice*. American Petroleum Institute, Washington, D.C. (1941)
- Lake, L. W.: *Enhanced Oil Recovery*, Prentice-Hall Inc, Upper Saddle River, ISBN: 0-13-281601-6 (1989)
- Lin, W., Tang, G.Q., Kovscek, A.R.: Sorption-induced permeability change of coal during gas-injection processes. *Reserv. Eval. Eng.* **11**(4), 792–802 (2008)
- McKee, C.R., Bumb, A.C., Koenig, R.A.: Stress-dependent permeability and porosity of coal. In: Fassett, J.E. (ed.) *Geology and Coal-Bed Methane Resources of the Northern San Juan Basin*, pp. 143–153. San Juan Basin, Colorado and New Mexico (1988)
- Mineral Planning Factsheet: Coal and Coalbed Methane, British Geological Survey, October (2006)
- Pan, Z., Connell, L.D., Camilleri, M.: Laboratory characterisation of coal reservoir permeability for primary and enhanced coalbed methane recovery. *Int. J. Coal Geol.* **82**, 252–261 (2010)
- Pan, Z., Connell, L.D.: Modelling permeability for coal reservoirs: a review of analytical models and testing data. *Int. J. Coal Geol.* **92**, 1–44 (2012)
- Reid, R.C., Prausnitz, J.M., Poling, B.E.: *The Properties of Gases and Liquids*, 4th edn. McGraw Hill Inc., New York (1987)
- Talu, O.: Needs, status, techniques and problems with binary gas adsorption experiments. *Adv Colloid Interface Sci* **76–77**, 227–269 (1998)
- Tanikawa, W., Shimamoto, T.: Klinkenberg effect for gas permeability and its comparison to water permeability for porous sedimentary rocks. *Hydrol. Earth Syst. Sci. Dis.* **3**(4), 1315–1338 (2006)
- Thomas, L.: *Coal Geology*. Wiley, England, pp. 79–106 and 260 (2002)
- Yang, R.T.: *Gas Separation by Adsorption Processes*. Butterworths Publishers, London (1987)